Summer Research 2023 Review Doc: A Hose of Mass Transferring Systems

Liam Keeley

Department of Physics, Colorado College, Colorado Springs, CO 80903

August 2, 2023

1 Introduction

This summer, I used results from COSMIC, a software used to simulate stellar populations, to understand the gravitational wave signal from a population of binary white dwarf systems in absolute gravitational wave magnitude–gravitational wave frequency space, which we refer to as KT diagrams. Beginning in Section 2, I will review the results of Ravi Kumar Kopparapu and Joel Tohline's 2006 paper (KT) [[1]], which set the framework for the study of gravitational wave sources in the context of KT diagrams. Then, in Section 3 I will discuss how I used COSMIC to gain an intuition for white dwarf binary systems evolve in a KT diagram by focusing on individual systems. In Section 4, I discuss the Tourmaline B galaxy population and common envelope evolution. In Section 5 I discuss results from the Agate fixed populations, and the potential usefulness of KT diagrams in studying Type Ia supernovae of carbon white dwarfs accreting helium material. I also describe the evolution of neutron star white dwarf systems off of the mass transfer branch because of natal kicks. In Section 6, I apply a naive signal to noise analysis to the Agate populations and discuss the results from Section 5 that will be visible to a four year LISA mission. Finally, in Section 7 I discuss our plans to expand the Agate fixed population to an Agate galaxy population.

2 Regions of Absolute Magnitude-Frequency Diagram

KT split the domain of all possible points in an Absolute Magnitude-Frequency Diagram into regions where we would expect to find double white dwarf systems detectable by future space based gravitational wave detectors. Important to their analysis and our results with COSMIC is the distinction between a detached binary and contact binary, and the evolution of these systems.

A detached binary system is one in which the component stars are mostly non-interacting, although they may interact tidally in some cases. The dominant mechanism in the evolution of these systems is the shedding of energy and angular momentum via radiation of gravitational waves. This results in the binary orbit shrinking due to loss of energy and circularizing due to loss of angular momentum. The detailed mathematical evolution of an inspiraling binary system is derived in [2], but generally it is important to note that the rate at which energy and angular momentum are lost increases quickly as the orbital frequency increases.

The gravitational wave frequency is half the orbital frequency of the system. If we assume our systems obeys Kepler's Third Law, then the orbital frequency is related to the separation by:

$$\Omega^2 = G\frac{M_{tot}}{a^3} \tag{1}$$

Where G is the universal gravitational constant, M_{tot} is the total mass of the system, a is the orbital separation, and Ω is the orbital frequency. The orbital angular momentum is then given by the equivalent one body problem with the reduced mass $\mu = \frac{m_a m_d}{M_{tot}}$:

$$J_{orb} = \frac{m_a m_d a^2}{M_{tot}}\Omega = \left(\frac{Ga}{M_{tot}}\right)^{\frac{1}{2}} m_a m_d, \tag{2}$$

Or, in terms of the gravitational wave frequency:

$$J_{orb} = \left(\frac{GM_{tot}^5}{\pi f_{gw}}\right)^{\frac{1}{3}} Q, \text{ where } Q = \frac{q}{(1+q)^2} \text{ and } q = \frac{m_d}{m_a} \tag{3}$$

The absolute gravitational wave magnitude rh_{norm} can be shown to take the form (see e.g. [1], [2]):

$$rh_{norm} = \frac{4G^3}{c^4}\frac{M_{tot}^5 Q^3}{J_{orb}^2} \tag{4}$$

Evidently, we can then eliminate J_{orb} in favor of f_{gw} to give rh_{norm} in terms of f_{gw}. When we do so, we find that in a KT-diagram, any system with the same component mass m_a and m_d will fall along a line of slope $\frac{2}{3}$. As f_{gw} is proportional to the orbital frequency, the position along the line depends on the orbital separation through Keppler's Third Law.

On an inspiral trajectory, it is only the orbital separation–and not the component masses–which changes in time. Therefore, the trajectories of inspiraling binary systems in a KT diagram will fall along these lines of slope $\frac{2}{3}$.

The other trajectories that are important to consider are those of semidetached mass transferring systems. While the evolution of such systems are in general tricky to describe, we can get a sense for what they will do by assuming that both mass and orbital angular momentum are conserved during mass transfer. The angular orbital momentum of a binary system is given by Equation (2), so its first time derivative is:

$$\dot{J_{orb}} = \left(\frac{G}{M_{tot}}\right)\frac{d}{dt}\left[a^{\frac{1}{2}} m_a m_d\right] \tag{5}$$

$$= \left(\frac{G}{M_{tot}}\right)\left[\frac{\dot{a}}{2a^{\frac{1}{2}}} m_a m_d + a^{\frac{1}{2}}\dot{m}_a m_d + a^{\frac{1}{2}} m_a \dot{m}_d\right] \tag{6}$$

Because mass is conserved, $\dot{m}_a = -\dot{m}_d$, and:

$$\dot{J_{orb}} = \left(\frac{G}{M_{tot}}\right)\left[\frac{\dot{a}}{2a^{\frac{1}{2}}} m_a m_d + a^{\frac{1}{2}}\dot{m}_d(m_a - m_d)\right] \tag{7}$$

Assuming that angular momentum is conserved, then $\dot{J_{orb}} = 0$, so:

$$\frac{\dot{a}}{2a^{\frac{1}{2}}}m_a m_d = -a^{\frac{1}{2}}\dot{m}_d m_a(1-\frac{m_d}{m_a}) \tag{8}$$

$$\frac{\dot{a}}{a} = -2(1-q)\frac{\dot{m}_d}{m_d}, \tag{9}$$

Because the donor is losing mass and, as will be discussed in further detail later in this section, $q < 1$ for all white dwarf binary systems, it follows that so long as orbital angular momentum is mostly conserved, the orbital separation will increase. Moreover, the component masses are not constant, so the trajectory will not simply be backwards along the original inspiral trajectory. Rather, as q is decreasing during mass transfer, Q will as well, and so for a given orbital frequency rh_{norm} will always be less for a system on its mass transfer trajectory as compared with its inspiral trajectory.

These insights, beyond being useful for building intuition about the gravitational wave signal for inspiral and mass transfering systems, also allow us to make our first restriction on where double white dwarf systems can be found in a KT diagram. Because the maximum mass of a white dwarf star is the Chandrasekhar mass $M_{ch} = 1.44M_\odot$ and the inspiral trajectories are always at higher rh_{norm} as compared with mass transferring systems, double white dwarf systems will only be found below the inspiral trajectory of a system where $m_a = m_d = M_{ch}$. KT define this as Boundary A.

To further constrain the domain in which double white dwarf systems might be found, we must understand when they transition from being on inspiral trajectories to being on mass transfer trajectories. This occurs when the separation between the two systems becomes sufficiently small that the accretor attains a gravitational influence over some mass which was originally gravitationally bound to the donor: this mass will then be ripped off the donor and eventually become a part of the accretor.

This can be put mathematically using the Roche Lobe model, as presented in Chapter 13 of [3]. We consider the potential function for a bit of mass m in a frame corotating with the binary system set up so that the origin is in the orbital plan and lies on the axis of rotation:

$$U(\vec{r}) = \frac{Gmm_a}{r_a} + \frac{mm_d}{r_d} + \frac{1}{2}\Omega^2(x^2+y^2) \tag{10}$$

Here, $\vec{r}$ is the position vector of our bit of mass, $r_a = |\vec{r} - \vec{r_a}|$ is the distance from m to m_a, $r_d = |\vec{r} - \vec{r_d}|$ is the distance from m to m_d, and (x^2+y^2) is the distance from m to the axis of rotation (note that the last term is a pseudo-potential due to the rotating reference frame used). The boundary between mass bound to m_1 and mass bound to m_2 is then the equipotential surface on which $U(\vec{r}) = 0$: this is shown in the orbital plane in Figure 1.

Now, we can precisely define what it means for mass transfer to begin. We define the Roche Lobe radius for each star to be the radius of a sphere which has the same volume as the volume enclosed by the equipotential surface of $U(\vec{r}) = 0$. Then, mass transfer via Roche Lobe Overflow begins when, through one process or another, the radius of the donor exceeds its Roche Lobe radius. Evidently, the Roche Lobe radius will depend in some way on the donor mass, the accretor mass, and the orbital separation (as well as the orbital frequency, but by Kepler's Third Law this is not independent of the orbital separation). While we would be hosed if we searched for an exact analytical equation for the Roche Lobe of a star in terms of these variables, it should in principle be possible to solve (numerically at the very least) for the Roche Lobe radius if we are

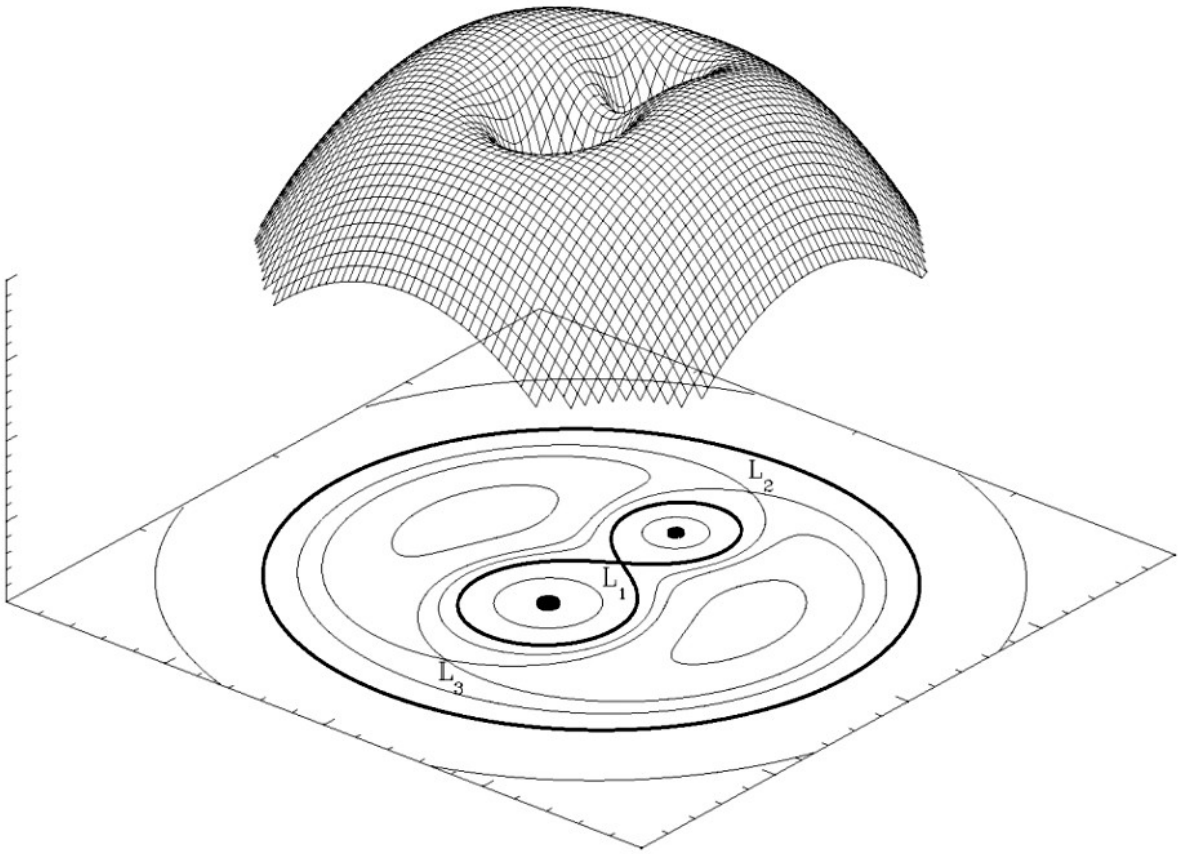

Figure 1: This shows surfaces of constant potential in the orbital plane for the potential function given by Equation (1). Surfaces of zero potential are bolded, and each of the two inner surface defines a volume: one around m_a and the other around m_d. The Roche Lobe radius for each star is defined as the radius of a sphere with the same volume as the volume enclosed by the surface of zero potential. Roche Lobe overflow will begin approximately when the donor's stellar radius exceeds the donor's Roche Lobe radius.

given these variables. Then, by solving for the Roche Lobe radius of many systems, we can fit a suitable analytical function to conveniently approximate the Roche Lobe radius, which is exactly what Eggleton did in 1983 (on his Apple II-plus computer) [5], giving the following semi-analytical formula for the Roche Lobe radius:

$$R_L \approx a \frac{0.49 q^{\frac{2}{3}}}{0.6 q^{\frac{2}{3}} + \ln\left(1 + q^{\frac{1}{3}}\right)} \tag{11}$$

This formula is valid for all binary systems (meaning all values of q, [5]). If we want to find the point at which Roche Lobe overflow begins specifically for white dwarfs, we can use the mass-radius relationship for a white dwarf is (as quoted in e.g. [1], [6]):

$$\frac{R_d}{R_\odot} = 0.0114 \left[\left(\frac{m_d}{M_{ch}}\right)^{-\frac{2}{3}} - \left(\frac{m_d}{M_{ch}}\right)^{\frac{2}{3}} \right]^{\frac{1}{2}} * \left[1 + 3.5 \left(\frac{m_d}{M_p}^{-\frac{2}{3}} \right) + \left(\frac{m_d}{M_p}\right)^{-1} \right]^{-\frac{2}{3}} \tag{12}$$

Where $M_p = 0.00057 M_\odot$ and $M_{ch} = 1.44 M_\odot$ is the Chandrasekar mass. Equation (11) and Equation (12) can be equated to give the orbital separation a at which mass transfer begins for a double white dwarf system. Note that this implies the less massive white dwarf will always donate mass to the more massive star: the more massive star will have a larger Roche Lobe and a smaller stellar radius, thus justifying our assumption that $q < 1$ for all double white dwarf binaries. This prescription is used by both the stellar evolution code BSE, which is used to evolve stars in COSMIC ([7], [8]), and by KT [1] to further constrain the region in which double white dwarf binaries will be found in a KT diagram. Notice that for a given accretor mass m_a, as we increase m_d, R_d decreases while q and R_L both increase. It follows that for two double white dwarf systems with the same total mass, the system with larger q will make it to large orbital frequencies before commencing mass transfer. This allows us to further constrain the region in which double white dwarf binaries will be found: no double white dwarf systems will be found below the curve defined by the point at which inspiral ends for all systems with $q = 1$. KT call this Boundary B.

These two curves define the region in which double white dwarf systems may be found in a KT diagram. We can split this region up further, although the boundaries become less concrete. A third boundary is given by the curve defined by the point at which inspiral ends for all systems with $m_a = M_{ch}$. KT claim that no mass transferring systems will be found to the left of this boundary, which is a helpful designation, although it can be misleading. For one, inspiraling systems will be found to the right of this line. Additionally, mass transferring systems can be found below the range of this line if the system's total mass is less than M_{ch}, which often turns out to be the case. Lastly, it actually is possible that mass transferring systems appear to the left of this line if there total mass is greater than M_{ch} and they have been mass transferring for some time. This line is still helpful at least for discussion; KT designate it Boundary C.

KT define two more boundaries based on where supernovae progenitors will be found. They derive these boundaries based on the mass ratio above which systems will enter unstable mass transfer upon beginning Roche Lobe Overflow and will coalesce soon thereafter. While this is a useful theoretical designation, in Section 5 we will extensively discuss systems which supernovae regardless of their initial q value, and so will limit our discussion to boundaries A, B, and C to avoid confusion.

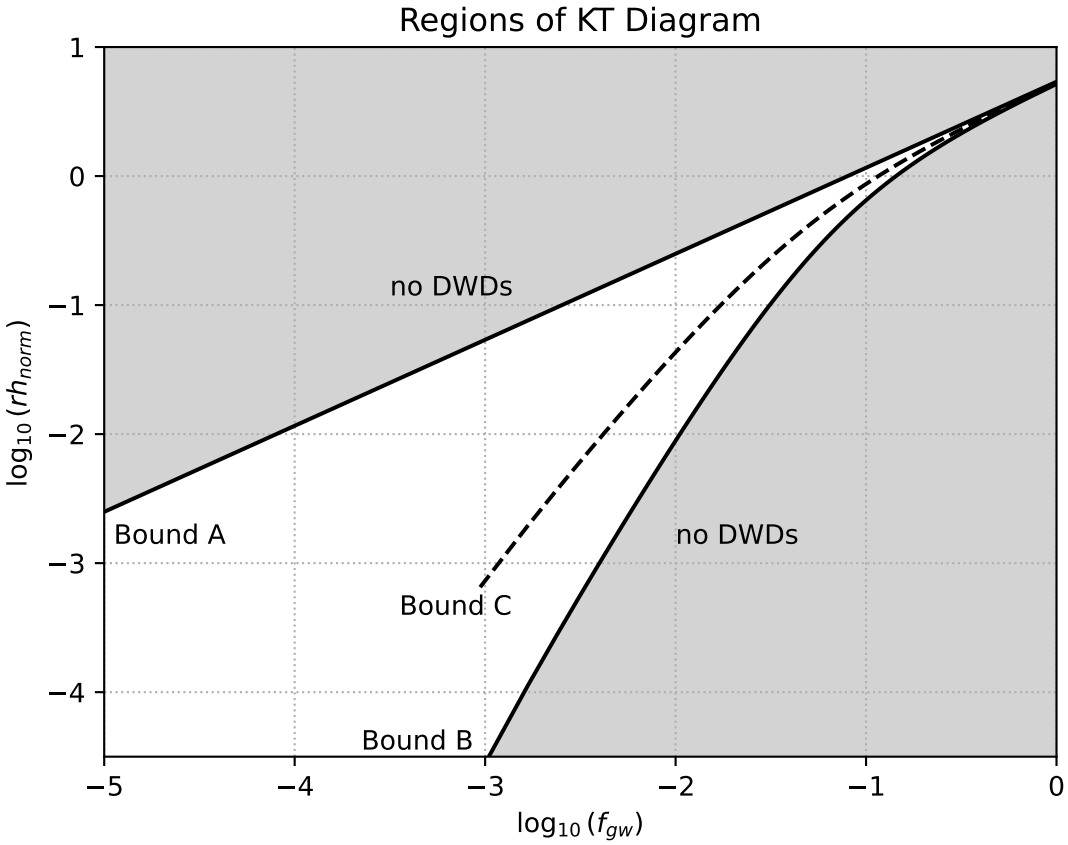

Figure 2: The general boundaries of a KT diagram we will discuss. Above Boundary A, which is the inspiral trajectory for a system with $m_a = m_d = M_{ch}$, no double white dwarf systems will be found. Below Boundary B, which is the locus of all points at which mass transfer begins for systems with $q = 1$, no double white dwarf systems will be found. While KT claim that no mass transferring double white dwarf systems will be found to the left of Boundary C–which is the point where mass transfer begins for all systems with $m_a = M_{ch}$–this is incorrect. Still, we keep it around for discussion.

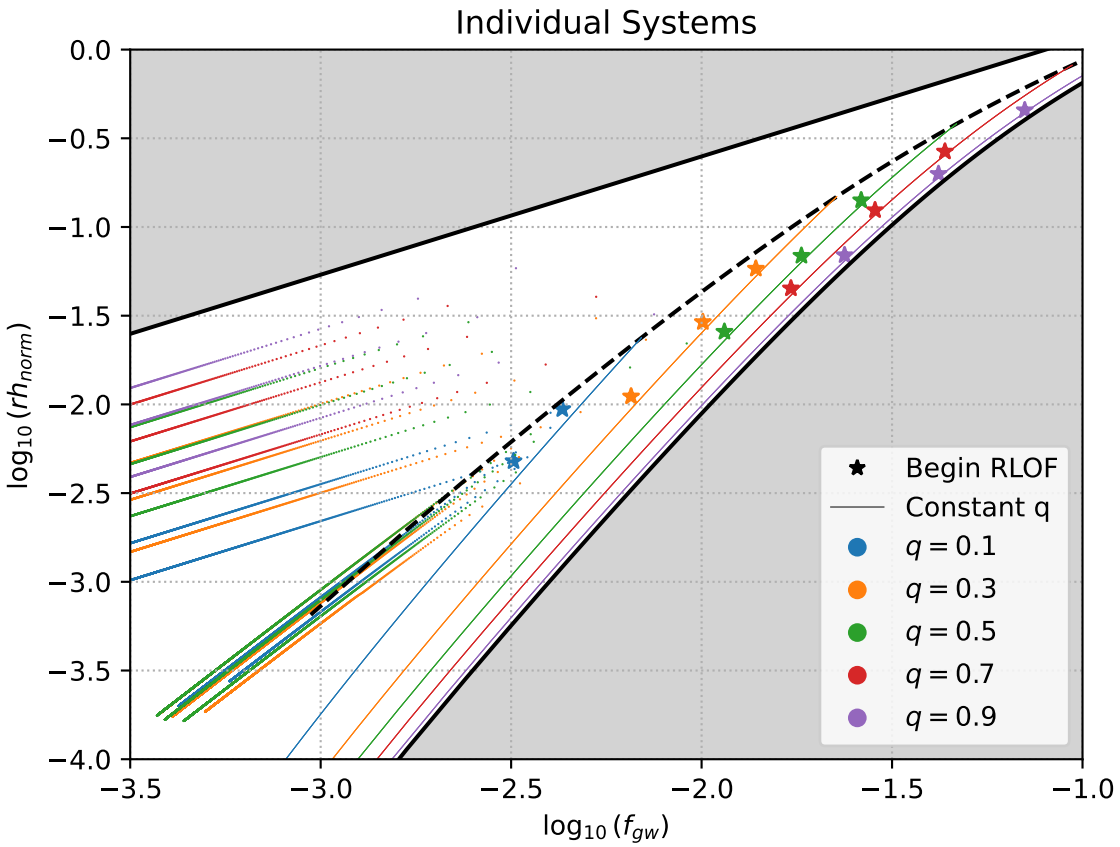

Figure 3: The individual evolutionary trajectories of individual systems in a KT diagram. We see that systems follow the expected inspiral trajectories, which end roughly where expected, although there seems to be some deviation for low mass systems which we have not investigated.

3 Tracking Individual Trajectories

To verify the predicted trajectories in KT, I used COSMIC to simulate several individual white dwarf binary systems to see how they evolve in time. We find that the the predicted trajectories are generally what we would expect: systems begin on slow inspirals, which speed up as the system eventually rushes towards mass transfer. After mass transfer begins, systems move–quickly at first–to smaller frequencies. However, they do not simply move back along their inspiral trajectories, but rather move on steeper slopes, and will be found at lower gravitational wave amplitudes as compared to where the same system was found on its inspiral trajectory.

Also, notice that Boundary C does not work as intended, and some mass transferring systems cross it even before its domain ends at $f_{gw} \approx 10^{-3}$. The difficulty with this boundary is that it is derived from considerations of when mass transfer begins, but systems are rarely observed near they begin mass transfer. Instead, they rush towards and away from this point, largely obscuring any structure that would otherwise be derived from information about when mass transfer begins.

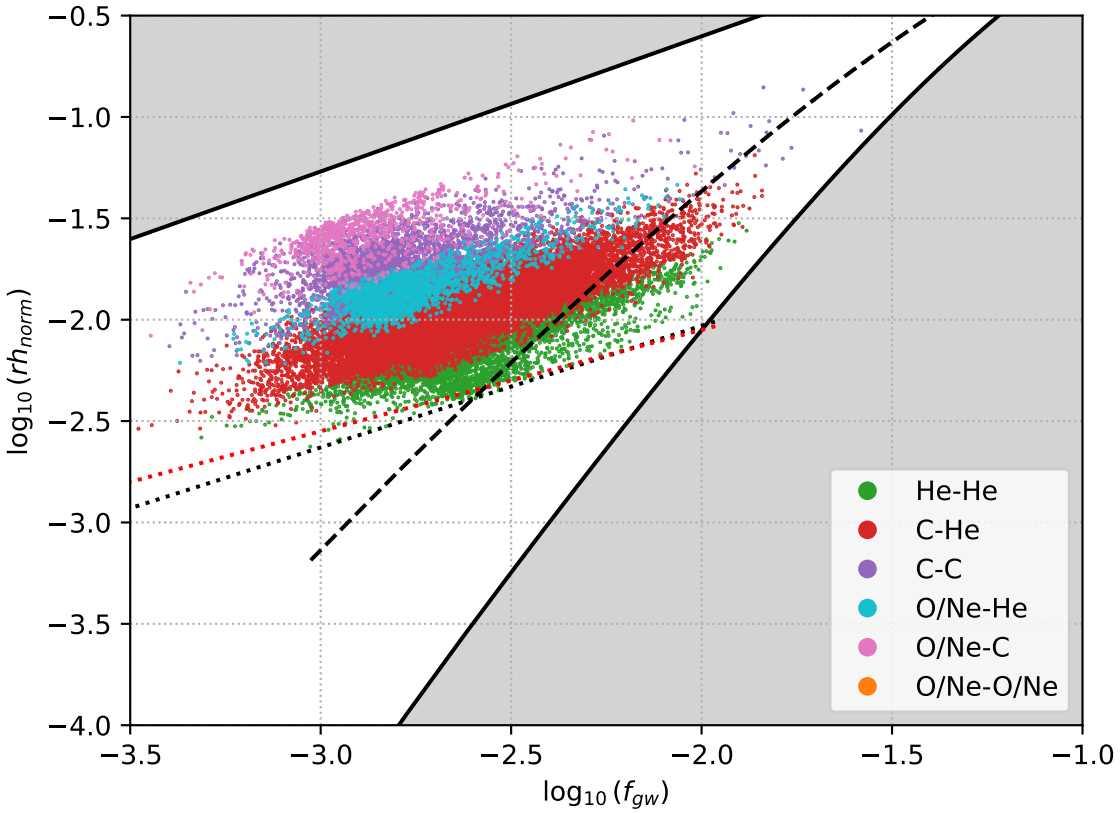

Figure 4: KT diagram for all resolvable source in the Tourmaline B galaxy population. Note, however, that the milky way maker code leaves out mass transferring systems, so we lose a lot of the structure we expect to see in a KT diagram. A constraing line fit to this date is show as a dotted black line, while the dotted red line is fit to systems coming out of common envelope evolution. Finally, this system has been filtered to show only sytems which will be obervable by LISA.

4 COSMIC Galaxy Results and Common Envelope Evolution

After getting a sense for the evolutionary trajectories of individual white dwarf binaries, I looked at some galaxy populations generated with COSMIC. These galaxy populations exclude mass transferring systems, a point which will be discussed in more detail in Section 5. The latest galaxy population produced, which we will discuss here, is the Tourmaline B galaxy.

We find that sources do separate by stellar type in a KT diagram, although there are significant regions of overlap. The observed separation is consistent with what we would expect based on the relative masses of white dwarfs of each stellar type. What is interesting is that there appears to be a cutoff below which no detached binaries are found. We can empirically fit a line to this cutoff, which is shown as a dotted black line in Figure 4. I hypothesized this cutoff was due to common envelope physics. For double white dwarfs to reach a point in their evolution where they are visible to LISA, they must undergo at least one period of common envelope evolution [9], and so

it seems reasonable that the details of which systems reach a phase of common envelope evolution could produce such a cutoff. While these details are poorly understood, it is described in BSE [8] and COSMIC [7] using the $\alpha\lambda$ prescription. In this prescription, only the initial gravitational potential energy of the common envelope and the final potential energy of the common envelope are considered, while the complicated details of how the envelope is expelled are ignored. Most often, the initial potential energy is taken to be the gravitational potential energy of the envelope when Roche Lobe overflow (RLOF) begins:

$$E_i = \frac{G m_d^e m_d}{\lambda R_{L1}} \tag{13}$$

By definition, when RLOF begins, the radius of the envelope will be R_{L1}, while m_d^e is the mass of the donor's envelope. Then, λ is a parameter which accounts for the distribution of mass within the envelope. The final energy is simply taken to be the gravitational potential energy of the envelope after it has been expelled: $E_f = 0$ so $\Delta E_{env} = -\frac{G m_d^e m_d}{\lambda R_{L1}}$.

The change in the orbital energy is given by:

$$\Delta E_{orb} = -\frac{G}{2}\left[\frac{m_d^c m_a}{a_f} - \frac{m_d m_a}{a_i}\right] \tag{14}$$

Where m_d^c is the mass of the donor's core–that is, the mass that remains after the envelope has been expelled. Finally, the change in the orbital energy is related to the change in the envelope energy by the efficiency parameter α:

$$\alpha = \frac{\Delta E_{env}}{\Delta E_{orb}} \tag{15}$$

Thus, we find that once α and λ have been chosen, the orbital separation after common envelope evolution depends fundamentally on the initial separation, the initial mass of the accretor and donor, and the mass of the donor's envelope when RLOF begins. The Roche Lobe radius is also important, but is not independent of these variables. If we were to try and find some sort of limiting system we would consider the interdependence of these variables, which are connected through the Red giant evolution of the secondary. This will not be attempted here because, as will be discussed shortly, we found little evidence that the cutoff is caused by common envelope evolution.

To test the hypothesis that common envelope evolution produces a cutoff below which inspiralling white dwarfs are absent, we investigated in more detail the evolution of He-He binary systems–which define the lower limit of systems in our galaxy population–in a KT diagram, as shown in Figure 5. We see that these systems do seem to fall along a semi-distinct line upon exiting common envelope evolution, which has been empirically fit (eye-balled). We have also shown this line in Figure 4 as a dotted red line. Evidently, the two cutoff line are different, and so we decided to leave a more detailed study of common envelope evolution for another summer. However, I do expect that considering different common envelope evolution parameters may still be an interesting application of KT diagrams and COSMIC. There may be less obvious ways in which observable features are altered which would show up in a fixed or galaxy population with altered common envelope features.

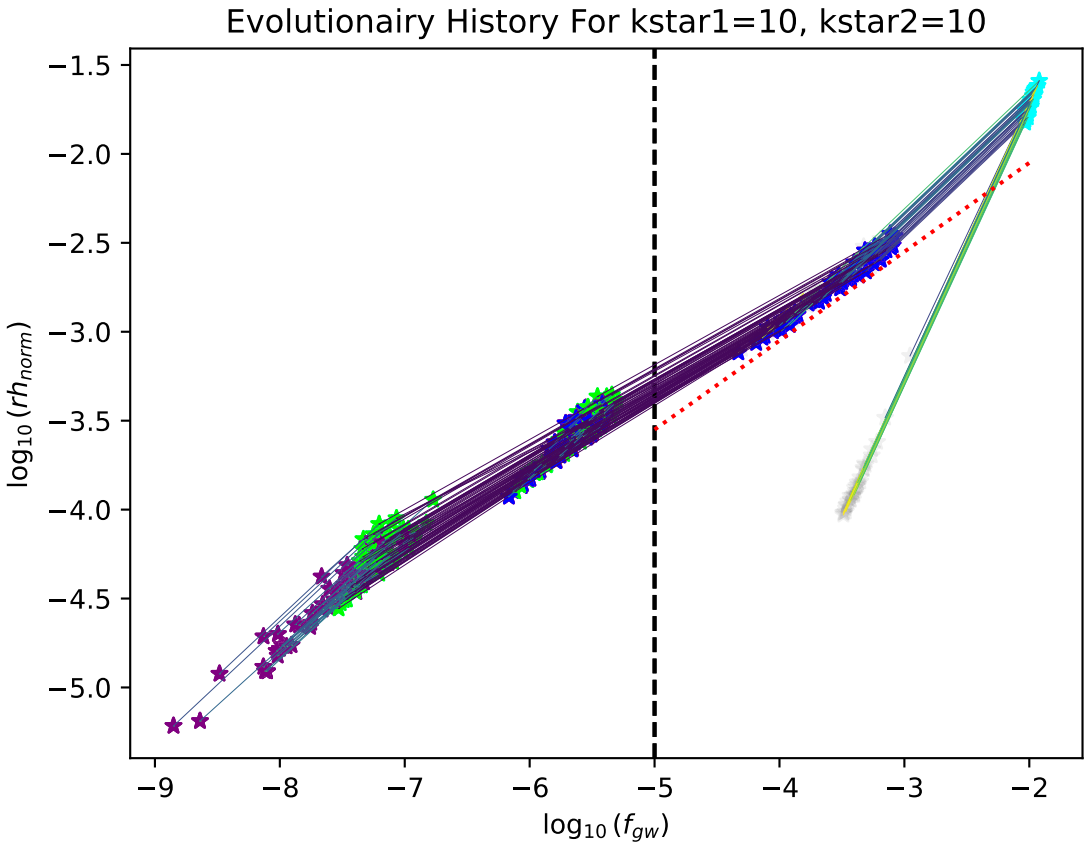

Figure 5: This shows the evolutionary trajectories over 13000 Myr for systems which end their evolution as double helium white dwarf systems. Plotted star symbols represent important events: purple for change of kstar, cyan for begin Roche Lobe Overflow, lime for begin common envelope, and blue for end common envelope. The color of lines between the important events represents the amount of time the system spent evolving on that segment, with dark purple being no time and lighter coloring being longer times. We see that all of these systems go through two phases of common envelope evolution which are instantaneous (dark purple) jumps in the diagram from lime stars to blue stars. The first phase of common envelope evolution occurs after the primary becomes a red giant and the second after the secondary becomes a red giant. We see that the two phases of common envelope evolution do seem to bring systems onto a line in the KT diagram; however, when we fit this line, we find that it does not constrain systems in the galaxy population as we had hoped. The last segment on the right is a long mass transfer trajectory onto which some systems make it, while the the segment before that is the inspiral trajectory which is the state of all systems in Figure 4

.

5 Mass Transferring Systems In KT Diagrams and the Agate Fixed Populations

The most interesting structure we expect to observe in KT diagrams occur due to the trajectories of semi-detached mass transferring systems; however, the current milky way maker code used to create COSMIC galaxy populations leaves them out. For this reason, in our study of mass transferring systems observable to LISA we are limited to fixed populations (at this time). To this end, I created nine fixed populations, three each for the bulge, thin disk, and thick disk which randomly and realistically sample the birth time of each star: between 9000 and 10000 Myr for the bulge, between 11000 and 10000 Myr for the thick disk, and between 10000 Myr and the present for the thin disk (I found these number in the Milky Way maker code; presumably there is a suitable paper citation, but I haven't gotten around to tracking it down). We refer to these populations as the Agate fixed populations. It should be noted that BSE does not account for direct impact accretion [8], which is important when considering a population of mass transferring systems [6], [10]. Moreover, Agate does not sample a proportional amount of mass from each system. Still, Agate provides a good starting point for understanding the structure and observability of mass transferring systems.

In Figure 6 I show all Agate systems by final evolutionary type, while in Figure 7 I show the same systems by the stellar makeup of the component stars. Referring to Figure 6, we see that we have three main groups: a primary grouping of inspiral trajectories, a secondary grouping of inspiral trajectories located below the primary grouping in the range $f_{gw} \in \{10^{-5}, 10^{-4.5}\}$ (these will not be visible with LISA), and a grouping of mass transfer trajectories mirroring those we found when studying individual systems.

Using diagrams similar to Figure 5, we discover that systems in different groupings–maybe not surprisingly–follow similar evolutionary paths. Systems in the primary inspiral branch are composed of a plethora of double white dwarf systems comprised of many different stellar components. While systems which have different stellar components have different evolutionary histories, systems within the primary grouping and which all have the same stellar components do have the same evolutionairy history. For all component types, at least one period of common envelope evolution is observed for all systems in the primary inspiral branch. This branch further separates as we would expect based on the relative masses of the systems, with heavier systems generally found at higher rh_{norm}.

The secondary grouping of insprial systems undergo one phase of common envelope evolution before the primary becomes a red giant, and then undergo a phase of stable mass transfer when the secondary is a red giant, which brings them down into their position below the main branch of inspiral trajectories. Only after this phase of stable mass transfer does the secondary become a white dwarf.

Finally, systems in the mass transferring branch follow the same trajectories as those in the main inspiral branch, but then reach the end of their inspiral trajectory and end up on their mass transfer trajectory where they are observed. The branch of mass transferring systems has a few systems with evolutionary type 2 and 4. These can both be explained. Those which end as evolutionary type 2 are in fact on mass transfer trajectories; however, they started out on those trajectories before the secondary became a white dwarf, so their final designation is evolutionary type 2 after the secondary becomes a white dwarf. Those that end as evolutionary type 4 are more interesting. The primaries of these systems accrete enough matter to exceed the Chandrasekhar mass, after

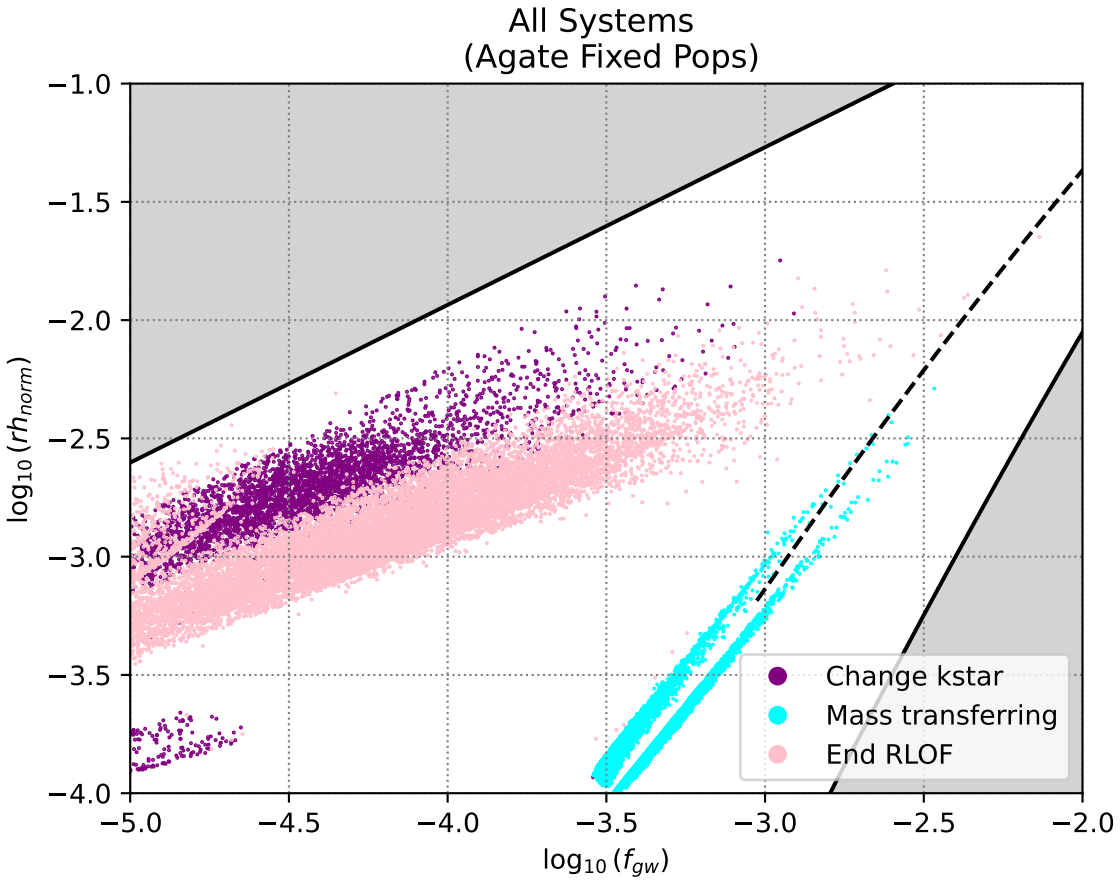

Figure 6: This KT diagram depicts all systems in the fixed populations for each of the bulge, thin disk, and thick disk. We find three general groupings: a primary inspiral branch, a secondary inspiral branch below it, and a mas transferring branch.

which the primary undergoes a partial supernova of the primary. This imparts a natal kick on the system, which acts to increase the orbital separation so that the secondary no longer fills its Roche Lobe, at which point RLOF ends. Comparing Figure 6 and Figure 7, we see that while there are many neutron star-white dwarf systems on the mass transfer branch, only a few get a large enough kick to end Roche Lobe overflow. These systems are observed far from the main mass transfer branch as we would expect.

Looking more closely at the mass transferring group, we find that there are actually two distinct groups with the lighter double helium systems forming the group at lower rh_{norm}, as we would expect. Noticeably missing among the mass transferring systems are carbon helium systems, which–based on their position on the inspiral branch–we expect would fill in the gap. The reason for these missing systems is given in [8]: while these systems are likely to begin stable mass transfer, after roughly $0.15M_{\odot}$ of helium has been accreted onto the carbon accretor, helium fusion ignites at the base of the accreted helium shell. This results in a pressure wave which propagates inwards: carbon briefly ignites off-center in the core resulting in an outward propagating detonation which destroys the star in a type Ia supernova. This process, however, is not fully understood, and [8] note that there is some thought that some Co-He systems would survive as mass transferring sys-

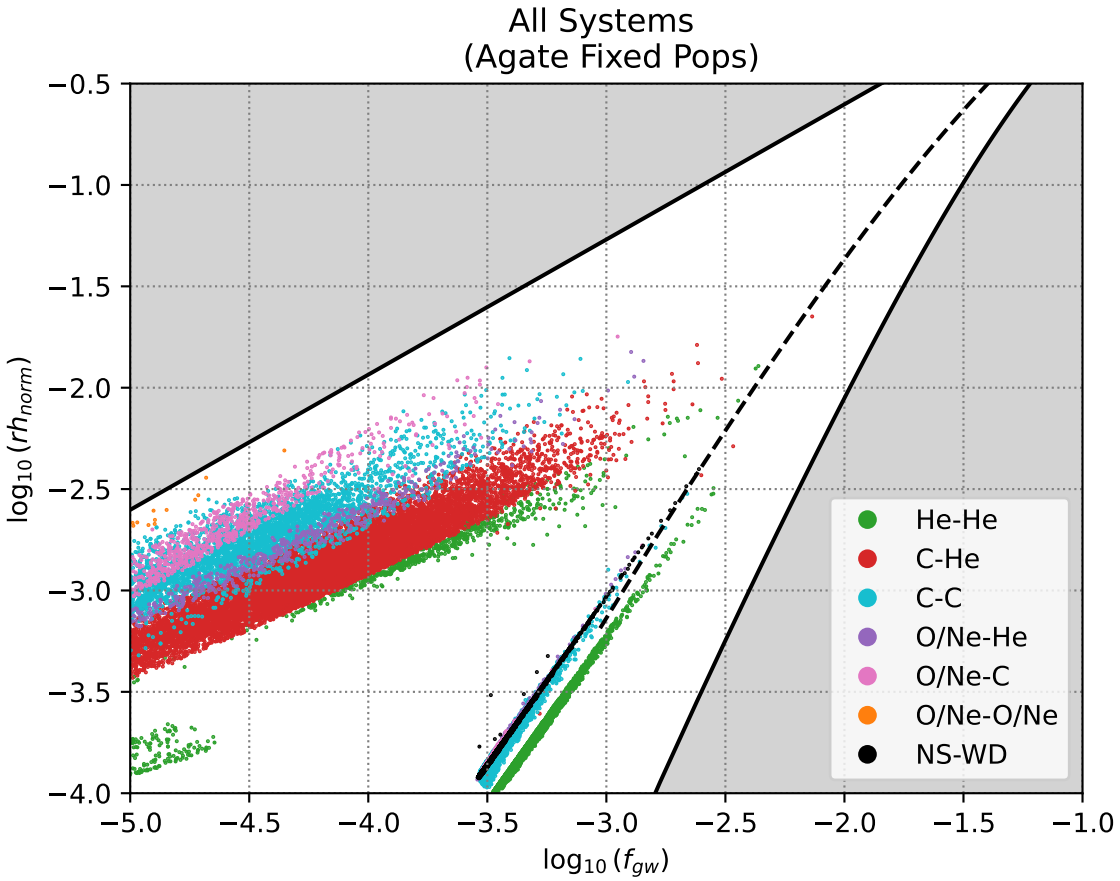

Figure 7: This figure depicts the same sources as Figure 6, except rather than the final evolutionairy type, it shows the stellar makeup of the systems in the diagram.

tems which would fill in the gap we observe. I have have not yet conducted a literature review of the subject, but [8] points to some starting points, although they are likely to be a bit dated. Regardless, this is point where LISA data will likely be useful in elucidating a part of stellar physics which is still only partially understood.

For the most part, systems of the same stellar components which are found at higher rh_{norm} on their inspiral trajectory are also found at higher rh_{norm} on their mass transfer trajectories. However, this is not the case for Oxygen Neon-Helium white dwarf systems. As can be seen Figure 8, Oxygen Neon-Helium systems are found at higher rh_{norm} as compared with carbon-carbon systems on the mass transfer branch, in contrast to the inspiral branch, in which we can see in Figure 7 that the carbon-carbon systems are generally found at higher rh_{norm}. We find while these systems are mostly found at lower rh_{norm} than Carbon-Carbon systems on the inspiral branch, the Oxygen Neon-Helium systems are found at higher rh_{norm} on the mass transfer branch. We propose that this is do to the initial mass ratios of carbon-carbon systems being nearer to one on the inspiral branch, but all systems approach a mass ratio of zero on the mass transfer branch, at which point the total mass is a larger factor in determining rh_{norm}.

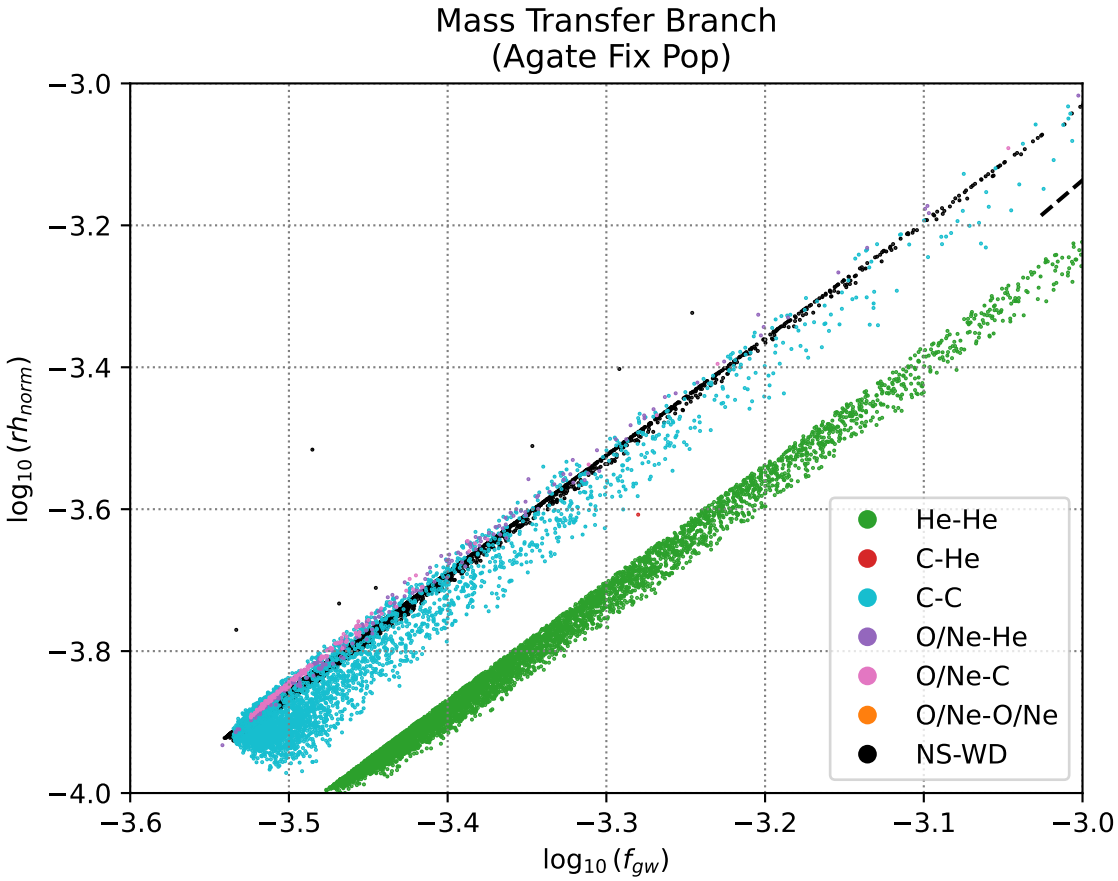

Figure 8: A zoomed in view of the end of the mass transfer branch of the Agate fixed population, where we can clearly see that oxygen-neon helium systems are generally found at greater rh_{norm} than carbon carbon systems, in contrast to the inspiral branch where carbon-carbon are the ones generally found at greater rh_{norm}.

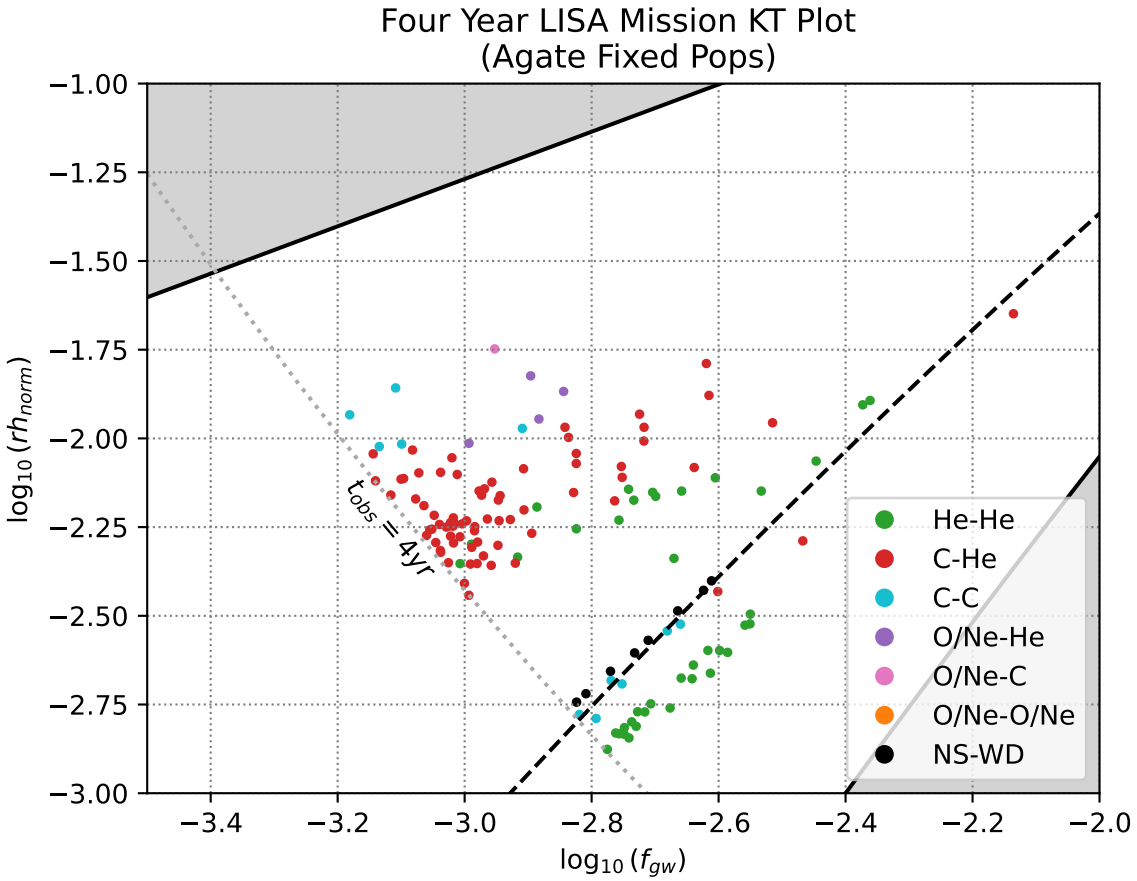

Figure 9: This figure shows systems in the Agate fixed populations which will be observable to a four year LISA mission, color coded by their stellar components. Notice that a number of neutron star white dwarf systems will be observable in the mass transferring branch.

6 Observability of Mass Transferring Systems

In this section, I apply signal to noise analysis to the Agate fixed populations to determine the observability of mass transferring systems. I make a number of assumptions in doing so. First, I assume all systems are at $8kpc$ from the detector. Secondly, I treat systems with signal to noise ratio greater than one as detectable, and those with signal to noise ratio less than one as undetectable, and I assume a four year mission length (maybe I'll make it 10–I'm an optimist). Finally, while we would expect many of these systems to be negatively chirping, I treat all systems as monochrome because it is unclear how to apply a more accurate analysis treating the chirping nature of mass transferring systems. For the mass transferring systems, this means that I overestimate the actual number of systems which will be observed: these systems are evolving towards frequencies with greater noise and towards lower rh_{norm}, so they are becoming less detectable.

Still, I think we can expect to observe a significant number of mass transferring systems, some of which will be neutron star white dwarf systems. While it is not immediately obvious if these will be distinguishable from double white dwarf systems, it is conceivable that the natal kick might put the system into an eccentric orbit. All the white dwarf systems will be in more or less circular

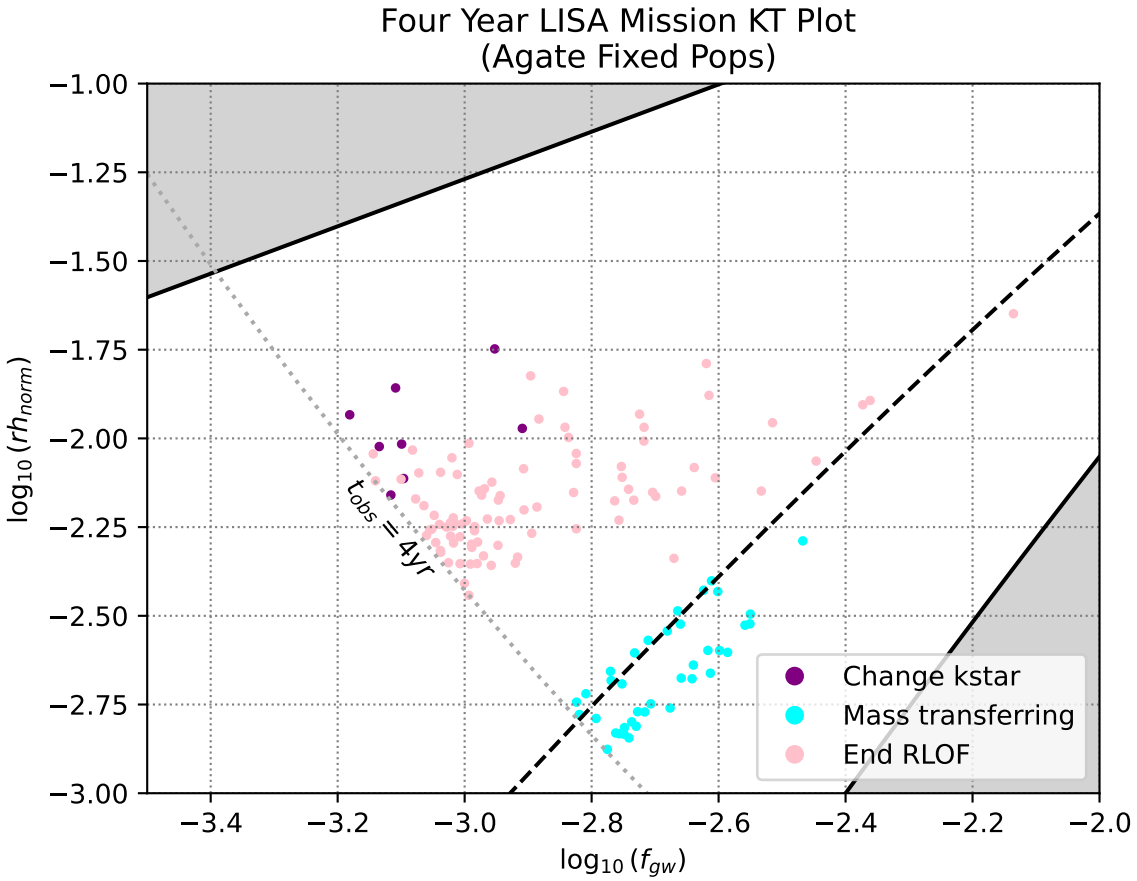

Figure 10: This figure shows systems in the Agate fixed populations which will be observable to a four year LISA mission, color coded by their final evolutionairy type. As we can see, a number of mass transferring systems should be observed

orbits as they are all near the end of their inspiral trajectory, so this would provide one way in which to distinguish the two. Otherwise, it's possible that a few large natal kicks will put some neutron stars onto their own branch where double white dwarf systems are otherwise not found, as we observed at the tail end of the mass transfer branch (which is cutoff after applying signal to noise analysis). It is difficult to describe exactly what will be detectable with only the relatively small Agate fixed populations.

7 The Agate Galaxy Population

Our investigations into the mass transfer branch the Agate fixed populations have demonstrated a number of possibilities for studying stellar physics with the binary systems which will be observable with LISA, including common envelope physics, type Ia supernovae due to the accretion of helium onto a carbon white dwarf, and the effect of natal kicks on neutron star-white dwarf binaries. However, the LISA sources we have studied in the Agate fixed population are only a small fraction of the sources which will be observable in an entire galaxy. On the one hand, we may be missing interesting systems which are rare enough to occur in a galaxy but not in our smaller

fixed populations. On the other hand, it may occur that the structure we are now observing will be confused by the multitude of all the systems which will be observable with LISA. For this reason, we are proceeding with the ambitious project of using COSMIC to produce a galaxy which will contain mass transferring systems. Unfortunately, this means we must evolve every binary system directly rather than using the convergence sampling method described in [7] (we need to be dumb instead of smart for a little bit, a task I am uniquely suited for). While it might seem that we would be properly hosing ourselves to attempt this with anything short of a supercomputer, I have a plan that I believe will work. Well, it is not so much a plan as seven iMacs and three months.

What I have done is make some minor changes to cosmic-pop so that rather than looping until convergence it simply loops until a certain amount of mass has been sampled. If we assume a bulge mass of $8.9 \times 10^9 M_\odot$, thick disk mass of $1.44 \times 10^{10} M_\odot$, and thin disk mass of $4.32 \times 10^{10} M_\odot$ (taken from galaxy maker code), and we assign one computer to the bulge, two to the thick disk, and the remaining four to the thin disk, my tests estimate that it will take between two and three months to produce a galaxy population. It is possible that we will in fact end up hosed, but I am optimistic that nobody really uses the physics iMacs (I have reached out to professors teaching the classes which might use them–they haven't got back to me so I'm pretty sure were good. Also, one of those classes I have taken and we never touched the iMacs and the other is block 4 so shouldn't present a problem anyhow. Worst case scenario we run it for the next month and finish up over winter break).

References

[1] Ravi Kumar Kopparapu and Joel Tohline. *Population Boundaries For Galactic White Dwarf Binaries in* LISA's *Amplitude-Frequency Domain.* The Astrophysical Journal, 655:1025–1032, 2007.

[2] P. C. Peters. "Gravitational Radiation and the Motion of Two Point Masses. *Physical Review,* Volume 136 Number 4b, July 1964.

[3] Benaquista, Mathew. *An Introduction to the Evolution of Single and Binary Stars,* Springer 2013.

[4] By Marc van der Sluys - http://hemel.waarnemen.com/Informatie/Sterren/hoofdstuk6.html#h6.2, CC BY 2.5, https://commons.wikimedia.org/w/index.php?curid=804238

[5] Eggleton, P.P.. "Approximations to the Radii of Roche Lobes", The Astrophysical Journal, 268, 368-369, 1983.

[6] T.R. Marsh, G. Nelemans, and D. Steeghs. "Mass transfer between double white dwarfs", *Monthly Notices of the Royal Astronomical Society.* 350, 113–128, 2004.

[7] Katelyn Breivik et. al.. "COSMIC Variance in Binary Population Synthesis". *The Astrophysical Journal*, 898:71 (14pp), 2020.

[8] Hurley J.R., Tout C.A., and Pols O.R.. "Evolution of Binary Stars and the Effect of Tides on Binary Populations". *Monthly Notices of the Royal Astronomical Society*, 1–36, 2002.

[9] Amaro-Seoane, P., Andrews, J., Arca Sedda, M. et al. Astrophysics with the Laser Interferometer Space Antenna. Living Rev Relativ 26, 2 (2023). https://doi.org/10.1007/s41114-022-00041-y

[10] Kyle Kremer et. al.. "Accreting Double White Dwarf Binaries: Implications For LISA", Preprint, 2018.